SUPPLEMENTAL DATA

Construct	Registry title	Registry number
P_y = Ubc, Gal4 = 0, P_x = none (Fig. 2)	Ubc-CFP	BBa_J176093
P_y = Ubc, Gal4 = 0, P_x = Ubc (Fig. 2)	Test miR-luc sensor 1	BBa_J176142
P_y = Ubc, Gal4 = 0, P_x = HPK (Fig. 2)	Test miR-luc sensor 2	BBa_J176143
P_y = Ubc, Gal4 = 0, P_x = CMV (Fig. 2)	Test miR-luc sensor 3	BBa_J176144
P_y = Ubc, Gal4 = 5, P_x = none (Fig. 2)	Ubc-5xGal4-CFP	BBa_J176095
P_y = Ubc, Gal4 = 5, P_x = Ubc (Fig. 2)	Test miR-luc sensor 4	BBa_J176145
P_y = Ubc, Gal4 = 5, P_x = HPK (Fig. 2)	Test miR-luc sensor 5	BBa_J176146
P_y = Ubc, Gal4 = 5, P_x = CMV (Fig. 2), Circuit 2 (Fig. 3B)	Test miR-luc sensor 6	BBa_J176147
P_y = Ubc, Gal4 = 10, P_x = none (Fig. 2)	Ubc-10xGal4-CFP	BBa_J176098
P_y = Ubc, Gal4 = 10, P_x = Ubc (Fig. 2)	Test miR-luc sensor 7	BBa_J176148
P_y = Ubc, Gal4 = 10, P_x = HPK (Fig. 2)	Test miR-luc sensor 8	BBa_J176149
P_y = Ubc, Gal4 = 10, P_x = CMV (Fig. 2)	Test miR-luc sensor 9	BBa_J176150
P_y = HPK, Gal4 = 0, P_x = none (Fig. 2)	HPK-CFP	BBa_J176092
P_y = HPK, Gal4 = 0, P_x = Ubc (Fig. 2)	Test miR-luc sensor 10	BBa_J176151
P_y = HPK, Gal4 = 0, P_x = HPK (Fig. 2)	Test miR-luc sensor 11	BBa_J176152
P_y = HPK, Gal4 = 0, P_x = CMV (Fig. 2)	Test miR-luc sensor 12	BBa_J176153
P_y = HPK, Gal4 = 5, P_x = none (Fig. 2)	HPK-5xGal4-CFP	BBa_J176096
P_y = HPK, Gal4 = 5, P_x = Ubc (Fig. 2)	Test miR-luc sensor 13	BBa_J176154
P_y = HPK, Gal4 = 5, P_x = HPK (Fig. 2)	Test miR-luc sensor 14	BBa_J176155

P_y = HPK, Gal4 = 5, P_x = CMV (Fig. 2)	Test miR-luc sensor 15	BBa_J176156
P_y = HPK, Gal4 = 10, P_x = none (Fig. 2)	HPK-10xGal4-CFP	BBa_J176091
P_y = HPK, Gal4 = 10, P_x = Ubc (Fig. 2)	Test miR-luc sensor 16	BBa_J176157
P_y = HPK, Gal4 = 10, P_x = HPK (Fig. 2), Circuit 1 (Fig. 3B), luc control circuit (Fig. 4A)	Test miR-luc sensor 17	BBa_J176158
P_y = HPK, Gal4 = 10, P_x = CMV (Fig. 2)	Test miR-luc sensor 18	BBa_J176159
P_y = CMV, Gal4 = 0, P_x = none (Fig. 2)	CMV-CFP	BBa_J176094
P_y = CMV, Gal4 = 0, P_x = Ubc (Fig. 2)	Test miR-luc sensor 19	BBa_J176160
P_y = CMV, Gal4 = 0, P_x = HPK (Fig. 2)	Test miR-luc sensor 20	BBa_J176161
P_y = CMV, Gal4 = 0, P_x = CMV (Fig. 2)	Test miR-luc sensor 21	BBa_J176162
P_y = CMV, Gal4 = 5, P_x = none (Fig. 2)	CMV-5xGal4-CFP	BBa_J176097
P_y = CMV, Gal4 = 5, P_x = Ubc (Fig. 2)	Test miR-luc sensor 22	BBa_J176163
P_y = CMV, Gal4 = 5, P_x = HPK (Fig. 2)	Test miR-luc sensor 23	BBa_J176164
P_y = CMV, Gal4 = 5, P_x = CMV (Fig. 2)	Test miR-luc sensor 24	BBa_J176165
P_y = CMV, Gal4 = 10, P_x = none (Fig. 2)	CMV-10xGal4-CFP	BBa_J176099
P_y = CMV, Gal4 = 10, P_x = Ubc (Fig. 2)	Test miR-luc sensor 25	BBa_J176166
P_y = CMV, Gal4 = 10, P_x = HPK (Fig. 2)	Test miR-luc sensor 26	BBa_J176167
P_y = CMV, Gal4 = 10, P_x = CMV (Fig. 2)	Test miR-luc sensor 27	BBa_J176168
miR-34 sensor + BCL2 target sites (data not shown)	miR-34 BCL2 sensor	BBa_J176139
miR-34 sensor + CCND1 target sites (Fig. 4A)	miR-34 CCND1 sensor	BBa_J176140
miR-34 sensor + CDK6 target sites (Fig. 4A)	miR-34 CDK6 sensor	BBa_J176141
miR-34 sensor + luc target sites + CFP-PEST (Fig. 4B)	miR-luc sensor 2PEST	BBa_J176169

| miR-34 sensor + CDK6 target sites + CFP-PEST (Fig. 4B) | miR-34 CDK6 sensor 2.0 | BBa_J176170 |
| MV8 (zeocin resistance vector) | pcDNA3.1+zeo | BBa_J176124 |

Table S1. Constructs and vectors. See the MIT Registry of Standard Biological Parts (http://partsregistry.org) for annotated sequences.
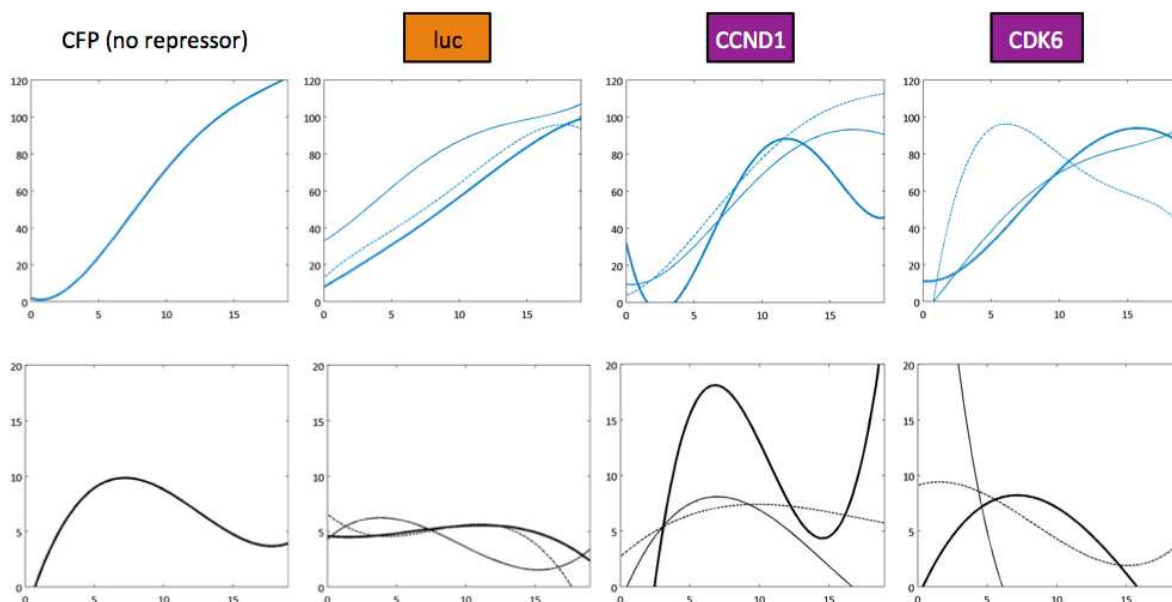

Figure S1. Regression curves for data shown in Figure 4A. Fourth degree polynomial best-fit curves for CFP output (top row, blue traces) were generated using MATLAB. The bottom row (black traces) are plots of the first derivative of the equations from the best fit curves. Line patterns correspond to the samples represented in Figure 4A. The first column of graphs, "CFP (no repressor)," were generated from averages of CFP expression from 5 individual cells, as a reference for the behavior of un-repressed CFP over time.
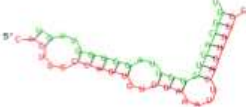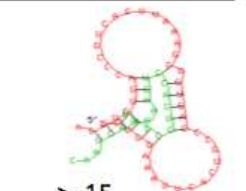
Figure S2. Free energies of miR-34/target site duplexes suggest significant differences in RNAi behavior. miR/target duplexes were predicted using RNAhybrid software. The duplexes with the lowest binding free energies are shown. The table lists average binding free energies ($\Delta G^{\circ}{}'$, kcal/mol) of all miR/target duplexes with $\Delta G^{\circ}{}' \leq 20$ kcal/mol, or the three most stable miR/target duplexes.

SUPPLEMENTAL MATERIALS AND METHODS

RNA hybridization analysis. miR-34/target duplex structures and corresponding binding free energies were predicted using the online software RNAhybrid (freely available at http://bibiserv.techfak.uni-bielefeld.de/rnahybrid/welcome.html).[1] This software was chosen for its speed, favorable reviews, and demonstrated predictive power in identifying physiological miR/target interactions.[2] Mature sequences of human miR-34a, miR-34b, and miR-34c were derived from miRBase (http://www.mirbase.org/), and were submitted to RNAhybrid for hybridization analysis against each target sequence used in the miR-34 sensor device. No user-defined structural or energetic constraints were used to limit the search space of potential interactions. Only miR-34/target duplexes with predicted binding free energies of $\Delta G^{\circ}{}' \leq 20$ kcal/mol[3-5] were used to calculate average binding free energies.

SUPPLEMENTAL REFERENCES

(1) Rehmsmeier, M.; Steffen, P.; Hochsmann, M.; Giegerich, R. Fast and effective prediction of microRNA/target duplexes. *RNA* **2004**, *10*, 1507–1517.
(2) Krüger, J.; Rehmsmeier, M. RNAhybrid: microRNA target prediction easy, fast and flexible. *Nucleic Acids Research* **2006**, *34*, W451–4.
(3) John, B.; Enright, A. J.; Aravin, A.; Tuschl, T.; Sander, C.; Marks, D. S. Human MicroRNA Targets. *PLoS Biol* **2004**, *2*, e363.
(4) Samols, M. A.; Skalsky, R. L.; Maldonado, A. M.; Riva, A.; Lopez, M. C.; Baker, H. V.; Renne, R. Identification of cellular genes targeted by KSHV-encoded microRNAs. *PLoS Pathog.* **2007**, *3*, e65.
(5) Ritchie, W.; Rajasekhar, M.; Flamant, S.; Rasko, J. E. J. Conserved expression patterns predict microRNA targets. *PLoS Comput. Biol.* **2009**, *5*, e1000513